



www.asianpubs.org

Asian Journal of Organic & Medicinal Chemistry

Volume: 5 Year: 2020
Issue: 4 Month: October–December
pp: 307–311
DOI: <https://doi.org/10.14233/ajomc.2020.AJOMC-P280>

Received: 28 June 2020
Accepted: 24 October 2020
Published: 31 December 2020

Author affiliations:

Department of Physics, Mrinalini Datta Mahavidyapith, Birati, Kolkata-700051, India

✉To whom correspondence to be addressed:

E-mail: biku.mdm@gmail.com

Available online at: <http://ajomc.asianpubs.org>

ARTICLE

DFT Based QSAR Studies of Phenyl Triazolinones of Protoporphyrinogen Oxidase Inhibitors

Bikash Kumar Sarkar[✉]

ABSTRACT

The quantitative structure activity relationships (QSARs) have been investigated on a series of substituted phenyl triazolinones having protoporphyrinogen oxidase (PPO) inhibition activities. The density functional theory (DFT) method is applied to calculate the quantum chemical descriptors. The derived QSAR model is based on three molecular descriptors namely highest occupied molecular orbital (HOMO) energy, electrophilic group frontier electron density (F_g^E) and nucleus independent chemical shift (NICS). The best QSAR model has a square correlation coefficient $r^2 = 0.886$ and cross-validated square correlation coefficient $q^2 = 0.837$.

KEYWORDS

Phenyl triazolinones, Protoporphyrinogen oxidase, QSAR, DFT.

INTRODUCTION

A highly prominent, attractive principle of herbicidal action is chlorophylls biosynthesis inhibition in plants. Protoporphyrinogen IX oxidase [1,2], which is a vital enzyme for chlorophylls biosynthesis, is the target for the action of various classes with distinct structures of a compound having high herbicidal activity, such as phenyl triazolinones, cyclic imides and diphenyl ethers [3,4]. These compounds exhibit the characteristics of good crop selectivity, low application rates, environmental safety and low residue, which are crucial for modern agrochemicals that have received a global research attention and resulted in the rapid and successful use of protoporphyrinogen oxidase (PPO) inhibitor as herbicides.

In a recent study [4], the phenyl triazolinones are reported as inhibitors of PPO. Many groups [5-7] tried to form the quantitative structure activity relationship (QSAR) to explain the PPO inhibition activity phenyl triazolinone series of molecules. Herein, density functional theory (DFT) [8-11] is used to generate the descriptors of QSAR equation. The highest occupied molecular orbital (HOMO) energy, electrophilic group frontier electron density (F_g^E) [12] and nucleus independent chemical shift (NICS) [13,14] of the molecules act as effective quantum chemical descriptors giving a very good QSAR model that satisfactorily explain the antimalarial activity for this class of molecules. This study is likely to provide useful guidelines for the design of new inhibitors with better activities.

EXPERIMENTAL

In the formation of QSAR, choice of descriptors is a very important step. Many descriptors are reported in the literature [12,14,15], among them, nucleus independent chemical shift (NICS), group frontier electron density (F_g) and HOMO energy have been seen to be the appropriate descriptors for the present set of molecules.

Nucleus independent chemical shift (NICS): Schleyer *et al.* [13] proposed the NICS method for estimating aromaticity by using the ring current strength. For an aromatic system, NICSs are acquired as the negative values of absolute magnetic shielding factors, represented as NICS(1) and NICS(0), where these are computed at the ring centroid and 1 Å above the ring centroid, respectively. Generally, the more negative are the NICSs, the higher is the ring aromaticity and *vice-versa*. Anti-aromaticity is indicated by a positive NICS. A non-aromatic system exhibits a near-zero NICS value. NICSs are measured using the current of π -aromatic ring systems; however, the ring current of σ -bonds contaminates the NICS(0) current strength. Therefore, NICS(1) values are considered more suitable because 1 Å above the centroid, the ring current mainly comprises π -electrons (Fig. 1). NICS(1) can be a suitable descriptor that represents π -interactions between drugs and proteins because it is a measure of the π -electron ring current of an aromatic system. Recently, to establish QSAR models for COX-2 inhibitors, Sarkar *et al.* [14] introduced NICS(1) as quantum chemical descriptors, for the first time.

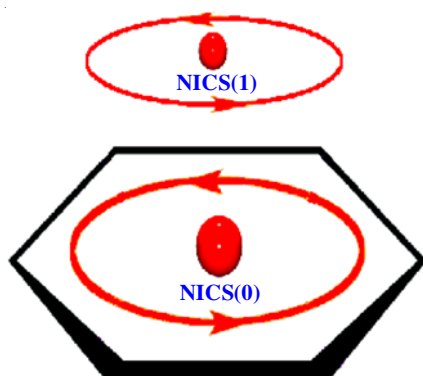


Fig. 1. Ring current on and above 1 Å an aromatic planar moiety. The strength of the current related to NICS(0) value on the ring and NICS(1) value above 1 Å

Group frontier electron density (F_g): The distribution of electrons associated with two frontier orbitals, namely HOMO and LUMO, is frontier electron density. HOMO and LUMO play a crucial role in various chemical reactions of unsaturated and saturated molecules thereby determine their reactivity. The two reactivity indices, electrophilic and nucleophilic frontier electron densities, were applied to evaluate the role of the electron density of frontier orbitals; Karelson *et al.* [15] introduced two reactivity indices, namely electrophilic frontier electron density (F_k^E) and nucleophilic frontier electron density (F_k^N), defined respectively as:

$$F_k^E = \frac{\sum (C_k^{\text{HOMO}})^2}{\Delta E} \times 100 \quad (1)$$

$$F_k^N = \frac{\sum (C_k^{\text{LUMO}})^2}{\Delta E} \times 100 \quad (2)$$

where, C_k^{HOMO} and C_k^{LUMO} are the coefficients of the atomic orbitals of any particular atom (kth) in HOMO and LUMO states, respectively. ΔE represents the energy gap between HOMO and LUMO.

The aforementioned frontier electron density definition is local, *i.e.* this definition considers single atom contribution in the electron density of frontier orbitals. Recently, we extended Karelson's definition of the density of frontier electrons to a set of atoms that are logically related (such as aromatic rings) belong to a larger molecule by defining the 'density of group frontier electrons', which is a sum of the densities of frontier electrons of a relevant class of atoms [13]. This new semi-global reactivity index is defined for a portion of molecules, which is also not based on atoms and not defined for an entire molecule. During intermolecular interactions, this index can provide the significance of the correlated atom set. According to the aforementioned definition of the density of group frontier electrons, two secondary reactivity indices were further introduced for the characterization of electrophilic and nucleophilic attacks, termed as electrophilic and nucleophilic group frontier electron densities, respectively. These are defined as:

$$F_g^E = \sum_{i=1}^n F_i^E \quad (3)$$

$$F_g^N = \sum_{i=1}^n F_i^N \quad (4)$$

where the summation is taken over a group of n relevant atoms.

Dataset selection and descriptor computation: Table-1 presents the activities of the protoporphyrinogen oxidase (PPO) inhibition of several phenyl triazolines derivatives acquired from the literature [4]. The selected molecule structures were completely optimised by employing the density functional theory (DFT) method [5-8] by using B3LYP/6-31G(d,p), the hybrid density functional of Becke's three parameters. It includes the DFT exchange correlation functional and Hartree-Fock exchange that used the Gaussian 03W program [16]. The optimized structures were investigated using harmonic vibrational frequencies, which indicated that the structures acquired were the minimal on the potential energy surface. Various descriptors of global and local reactivities were determined using the geometries optimised through Gaussian 03.

The NICSs were measured using the optimized geometries of molecules by employing the GIAO technique as executed in Gaussian 03. The densities of group frontier electrons (F_g^E , F_g^N) were determined using eqns. 3 and 4 by calculating the sum of the densities of frontier electrons of the atoms of a triazolone ring.

Model derivation and validation: A training set was used to derive QSAR models through multiple linear regression (MLR) by employing the observed antimalarial activities and different combinations of selected descriptors as dependent and independent variables, respectively. According to the data point number (n), standard error estimate (SEE), square of correlation coefficient (r^2), F-statistics (F), population (p), and T-statistics (T), model quality was considered statistically satis-

TABLE-1
MOLECULAR STRUCTURE FORMULA AND THEIR HERBICIDAL ACTIVITIES OF PHENYL TRIAZOLINONE DERIVATIVES

No.	R ₁	R ₂	pIC ₅₀	No.	R ₁	R ₂	pIC ₅₀
1	Cl	OCH ₂ CCH	7.6	12	Cl	Br	6.5
2	Cl	OCH ₂ CHCH ₂	7.5	13	Cl	C ₆ H ₅	6.3
3	Cl	OH	7.2	14	Cl	O-(4-NHSO ₂ Et)phenyl	6.6
4	Cl	CH ₂ OCH ₃	7.1	15	Cl	O-(4-methoxy)phenyl	6.7
5	Cl	NHSO ₂ C ₂ H ₅	7.1	16	Cl	O-(4-Cl)phenyl	6.7
6	Cl	OCOCH ₃	7.1	17	Cl	O-(4-NO ₂)phenyl	6.8
7	Cl	CH ₃	7.0	18	O-(4-Cl)benzyl	NH ₂	4.9
8	Cl	H	6.8	19	O-(4-Cl)benzyl	Cl	5.0
9	Cl	NHSO ₂ CH ₃	6.7	20	Br	H	6.1
10	Cl	OC ₆ H ₅	6.6	21	NO ₂	H	5.2
11	Cl	Cl	6.5	22	OCH(CH ₃)	H	5.1

factory. The large values of F indicate the model fit as not being a chance occurrence. The T-test was employed to determine the statistical significance of regression coefficients. Larger T-test values corresponded to regression coefficients with higher significance.

The acquired models were validated by measuring the coefficients of cross-validated squared correlation (q^2), which were determined using the 'leave-one-out' (LOO) test [17,18]. Many researchers [19,20] have considered higher q^2 value (> 0.5) as an indicator for a high-predictive QSAR models. By following procedures reported by Roy *et al.* [21], the QSAR models derived using the training set was employed to acquire the prediction of the biological activity of external test sets of seven molecules for evaluating the potential of external predictions [21].

RESULTS AND DISCUSSION

Derivation and validation of the model: To ascertain the relationship between chemical structures of selected phenyl triazolines derivatives and their protoporphyrinogen oxidase (PPO) inhibition activities (pIC₅₀) values, we have generated various equations through different combinations of DFT based local and global reactivity descriptors. It was kept in mind that for the best QSAR model the number of descriptors should be as small as possible and should have maximum correlation coefficient for the measured activities. In the present case, the best model was obtained using the descriptors (i) energy of highest occupied molecular orbital (HOMO), (ii) nucleus independent chemical shift (NICS) at aromatic ring and (iii) electrophilic group frontier electron density at the triazolone ring. The model having the highest correlation coefficient is:

$$\text{pIC}_{50} = -3.523 - 0.037 \text{ HOMO} - 0.526 \text{ NICS}(1) - 0.00426 F_g^E \quad (5)$$

with $n = 22$, $r^2 = 0.886$, $q^2 = 0.837$, $P = 0.000$, $F = 97.19$, $\text{SEE} = 0.171$.

Other relevant statistical parameters have been listed in Table-2. The Pearson correlation matrix (Table-3) shows that the descriptors are independent. The predicted pIC₅₀ values of

TABLE-2
UNCERTAINTIES, T-TEST AND P VALUES OF THE QSAR MODEL

Variables	Uncertainties	T-test values	P values
Constant	0.70	-4.34	0.000
HOMO	0.0025	-10.62	0.000
NICS(1)	0.062	-10.28	0.000
F_g^E	0.00031	-8.63	0.000

TABLE-3
PEARSON CORRELATION MATRIX

	pIC ₅₀	HOMO	NICS (1)	F_A^E
pIC ₅₀	1.000			
HOMO	-0.620	1.000		
NICS(1)	-0.530	0.005	1.000	
F_g^E	-0.680	0.023	-0.035	1.000

the training set and test set from the QSAR model is given in Table-2 along with actual measured activity values. A graph of actual activity versus predicted pIC₅₀ of the training set and test set has been provided in Fig. 2.

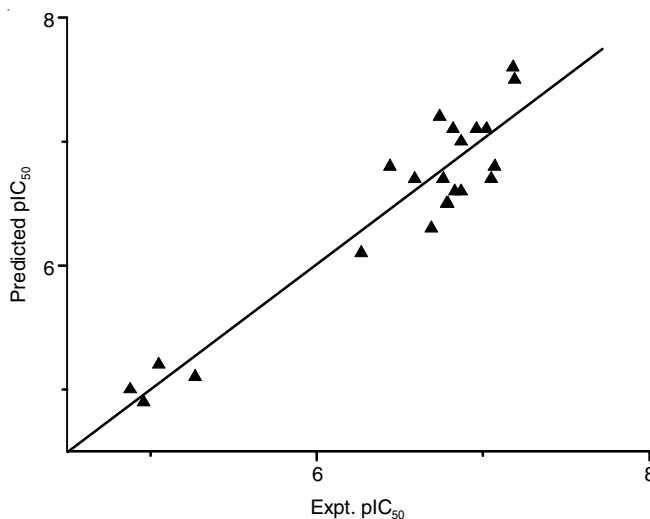


Fig. 2. Plot of predicted [from eqn. (1)] vs. experimental pIC₅₀

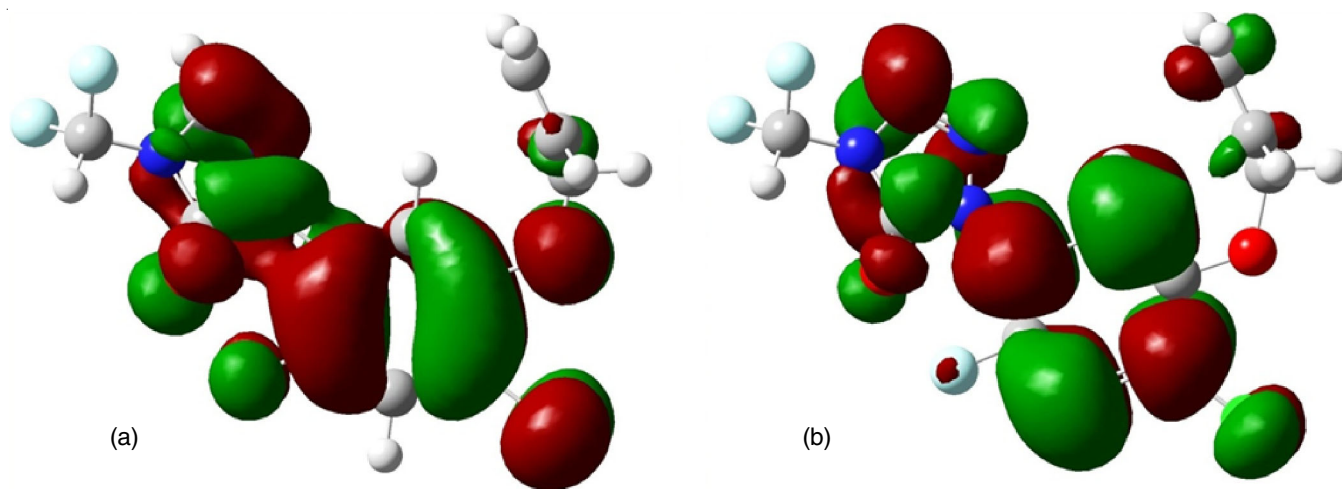


Fig. 3. (a) HOMO and (b) LUMO of molecule 1

From eqn. 5, it is obvious that NICS(1) of aromatic ring is the most important determining factor of the antimalarial activity. The NICS(1) values being itself negative and the coefficient of the NICS(1) term being the largest in eqn. 5, a higher magnitude of NICS(1) creates a positive contribution to the pIC_{50} values and thus is likely to be responsible for the antimalarial activity of the present set of molecules. Also, an electron releasing group at R_3 is likely to increase the NICS(1) value of aromatic ring. From Table-1, one can see that all sulfonyloxy group bearing molecules show comparatively higher activities. Being an electron releasing group, sulfonyloxy group increases the electron density on ring B and thus a higher value of the NICS(1) is induced by this group.

The group frontier electron density of triazolone ring is the least important among the descriptors as the coefficient multiplying it in eqn. 5 is hundred times smaller than the other coefficients. Group frontier electron density itself being positive, a high value of it tends to decrease the pIC_{50} . The electron density of triazolone ring can be increased by substituting the electron releasing groups at R_1 and R_2 . The HOMO and LUMO of the molecules are mainly located on aromatic and triazolone rings (Fig. 3) and partly on R_1 and R_2 . HOMO energy being negative a high value of HOMO energy will make a positive contribution to the activity.

Conclusion

In present work, the effectiveness of phenyl triazolones derivatives as potential protoporphyrinogen oxidase (PPO) inhibitors as herbicidal products was studied. The quantitative structure activity relationship studies based on DFT optimized structures of the molecules reveal that NICS(1) on the aromatic ring, electrophilic group frontier electron density and HOMO energy of the molecules are appropriate descriptors. It can be predicted that the baseborn of phenyl triazolone with NO_2 , CCl_3 , CF_3 as R_1 and NH_2 , NHR , OH , NR_2 ($R = \text{alkyl}$) as R_2 exhibit good activity.

REFERENCES

1. M. Matringe, J.M. Camadro, P. Labbe and R. Scalla, Protoporphyrinogen Oxidase as a Molecular Target for Diphenyl Ether Herbicides, *Biochem. J.*, **260**, 231 (1989); <https://doi.org/10.1042/bj2600231>
2. D.A. Witkowski and B.P. Halling, Inhibition of Plant Protoporphyrinogen Oxidase by the Herbicide Acifluorfen-Methyl, *Plant Physiol.*, **90**, 1239 (1989); <https://doi.org/10.1104/pp.90.4.1239>
3. J.W. Lyga, R.M. Patera, M.J. Plummer, B.P. Halling and A. Yuhas, Synthesis, Mechanism of Action, and QSAR of Herbicidal 3-Substituted-2-aryl-4,5,6,7-tetrahydroindazoles, *Pestic. Sci.*, **42**, 29 (1994); <https://doi.org/10.1002/ps.2780420106>
4. G. Theodoridis, Structure-Activity Relationships of Herbicidal Aryltriazolinones, *Pestic. Sci.*, **50**, 283 (1997); [https://doi.org/10.1002/\(SICI\)1096-9063\(199708\)50:4<283::AID-PS600>3.0.CO;2-L](https://doi.org/10.1002/(SICI)1096-9063(199708)50:4<283::AID-PS600>3.0.CO;2-L)
5. J. Wan, L. Zhang and G. Yang, Quantitative Structure-Activity Relationships for Phenyl Triazolones of Protoporphyrinogen Oxidase Inhibitors: A Density Functional Theory Study, *J. Comput. Chem.*, **25**, 1827 (2004); <https://doi.org/10.1002/jcc.20122>
6. K. Roy and S. Paul, Docking and 3D QSAR Studies of Protoporphyrinogen Oxidase Inhibitor 3H-Pyrazolo[3,4-d][1,2,3]triazin-4-one Derivatives, *J. Mol. Model.*, **16**, 137 (2010); <https://doi.org/10.1007/s00894-009-0528-8>
7. D. Wang, R.B. Zhang, I. Ismail, Z.Y. Xue, L. Liang, S.Y. Yu, X. Wen and Z. Xi, Design, Herbicidal Activity and QSAR Analysis of Cycloalka-[d]quinazoline-2,4-dione Benzoxazinones as Protoporphyrinogen IX Oxidase Inhibitors, *J. Agric. Food Chem.*, **67**, 9254 (2019); <https://doi.org/10.1021/acs.jafc.9b02996>
8. R.G. Parr, Density Functional Theory, *Annu. Rev. Phys. Chem.*, **34**, 631 (1983); <https://doi.org/10.1146/annurev.pc.34.100183.003215>
9. R.G. Parr and W. Yang, Density-Functional Theory of the Electronic Structure of Molecules, *Annu. Rev. Phys. Chem.*, **46**, 701 (1995); <https://doi.org/10.1146/annurev.pc.46.100195.003413>
10. H. Chermette, Chemical Reactivity Indexes in Density Functional Theory, *J. Comput. Chem.*, **20**, 129 (1999); [https://doi.org/10.1002/\(SICI\)1096-987X\(19990115\)20:1<129::AID-JCC13>3.0.CO;2-A](https://doi.org/10.1002/(SICI)1096-987X(19990115)20:1<129::AID-JCC13>3.0.CO;2-A)
11. P. Geerlings, F. De Proft and W. Langenaeker, Conceptual Density Functional Theory, *Chem. Rev.*, **103**, 1793 (2003); <https://doi.org/10.1021/cr990029p>
12. A. Sarkar, T.R. Middy and A.D. Jana, *J. Mol. Model.*, **18**, 2621 (2012); <https://doi.org/10.1007/s00894-011-1274-2>
13. P. von Rague Schleyer, C. Maerker, A. Dransfeld, H. Jiao and N.J.R. van Eikema Hommes, Nucleus-Independent Chemical Shifts: A Simple and Efficient Aromaticity Probe, *J. Am. Chem. Soc.*, **118**, 6317 (1996); <https://doi.org/10.1021/ja960582d>
14. A. Sarkar and G. Mostafa, A QSAR Study of Radical Scavenging Antioxidant Activity of a Series of Flavonoids using DFT Based Quantum Chemical Descriptors-The Importance of Group Frontier Electron Density, *J. Mol. Model.*, **15**, 1221 (2009); <https://doi.org/10.1007/s00894-009-0481-6>

15. M. Karelson, V.S. Lobanov and A.R. Katritzky, Quantum-Chemical Descriptors in QSAR/QSPR Studies, *Chem. Rev.*, **96**, 1027 (1996); <https://doi.org/10.1021/cr950202r>
16. M. Frisch, G.W. Trucks, H.B. Schlegel, G.E. Scuseria, M.A. Robb, J.R. Cheeseman, G. Scalmani, V. Barone, B. Mennucci, G.A. Petersson, H. Nakatsuji, M. Caricato, X. Li, H.P. Hratchian, A.F. Izmaylov, J. Bloino, G. Zheng, J.L. Sonnenberg, M. Hada, M. Ehara, K. Toyota, R. Fukuda, J. Hasegawa, M. Ishida, T. Nakajima, Y. Honda, O. Kitao, H. Nakai, T. Vreven, J.R. Montgomery Jr., J.E. Peralta, F. Ogliaro, M. Bearpark, J.J. Heyd, E. Brothers, K.N. Kudin, V.N. Staroverov, R. Kobayashi, J. Normand, K. Raghavachari, A. Rendell, J.C. Burant, S.S. Iyengar, J. Tomasi, M. Cossi, N. Rega, J.M. Millam, M. Klene, J.E. Knox, J.B. Cross, V. Bakken, C. Adamo, J. Jaramillo, R. Gomperts, R.E. Stratmann, O. Yazyev, A.J. Austin, R. Cammi, C. Pomelli, J.W. Ochterski, R.L. Martin, K. Morokuma, V.G. Zakrzewski, G.A. Voth, P. Salvador, J.J. Dannenberg, S. Dapprich, A.D. Daniels, O. Farkas, J.B. Foresman, J.V. Ortiz, J. Cioslowski and D.J. Fox, Gaussian Inc., Wallingford, CT (2009).
17. A. Golbraikh, M. Shen, Z. Xiao, Y.D. Xiao, K.H. Lee and A. Tropsha, Rational Selection of Training and Test Sets for the Development of Validated QSAR Models, *J. Comput. Aided Mol. Des.*, **17**, 241 (2003); <https://doi.org/10.1023/A:1025386326946>
18. D.M. Hawkins, S.C. Basak and D. Mills, Assessing Model Fit by Cross-Validation, *J. Chem. Inf. Comput. Sci.*, **43**, 579 (2003); <https://doi.org/10.1021/ci025626i>
19. B.F. Thomas, D.R. Compton, B.R. Martin and S.F. Semus, Modeling the Cannabinoid Receptor: A Three-dimensional Quantitative Structure-Activity Analysis, *Mol. Pharmacol.*, **40**, 656 (1991).
20. A. Agarwal, P.P. Pearson, E.W. Taylor, H.B. Li, T. Dahlgren, M. Herslof, Y. Yang, G. Lambert, D.L. Nelson, J.W. Regan and A.R. Martin, Three-Dimensional Quantitative Structure-Activity Relationships of 5-HT Receptor Binding Data for Tetrahydropyridinylindole Derivatives: A Comparison of the Hansch and CoMFA Methods, *J. Med. Chem.*, **36**, 4006 (1993); <https://doi.org/10.1021/jm00077a003>
21. P.P. Roy and K. Roy, On Some Aspects of Variable Selection for Partial Least Squares Regression Models, *QSAR Comb. Sci.*, **27**, 302 (2008); <https://doi.org/10.1002/qsar.200710043>